Research Square

Preprints are preliminary reports that have not undergone peer review.
They should not be considered conclusive, used to inform clinical practice,
or referenced by the media as validated information.

Surrogate Model based NSGA-II for Suspension Optimization for Two-Wheelers

Chirag Shrestha

chiragshrestha1999@gmail.com

Sikkim Manipal University https://orcid.org/0009-0008-9551-0244

Research Article

Keywords: Surrogate Modeling, Optimization, NSGA-II, Half-car Model

Posted Date: October 29th, 2026

DOI: https://doi.org/10.21203/rs.3.rs-10992219/v1

License: This work is licensed under a Creative Commons Attribution 4.0 International License.
Read Full License

Additional Declarations: The authors declare no competing interests.

Surrogate Model based NSGA-II for Suspension Optimization for Two-Wheelers.

Chirag G Shrestha[1*], Ranjan Pandey[1], Able Khanal[1], Anmol Shrestha[1], Manu Aryal[1].

[1]Yatri Motorcycles, Kathmandu, Nepal

*Corresponding Author: Chirag G Shrestha, chirag.shrestha@yatrimotorcycles.com

Abstract

Optimizing two-wheeler suspension systems for rider comfort traditionally requires computationally expensive dynamic simulations. This paper presents an efficient framework combining Kriging surrogate modeling with the Non-dominated Sorting Genetic Algorithm II (NSGA-II) to optimize suspension parameters on a two-wheeler. To bypass costly continuous MATLAB evaluations, a surrogate model is trained on a 4-DOF half-car model, mapping the non-linear relationships between front/rear stiffness, damping coefficients, and dynamic responses. NSGA-II is deployed across this surrogate space to search for parameters that minimize sprung mass vertical and rotational acceleration while satisfying constraints of vehicle stance, and suspension travel limits. The proposed surrogate-assisted methodology reduced computational time by 419% compared to traditional numerical integration while successfully identifying a Pareto-optimal front. The selected optimal configuration yielded a 16% improvement in rider comfort, providing a robust, time-efficient approach to fine-tuning two-wheeler suspensions.

Keywords: Surrogate Modeling, Optimization, NSGA-II, Half-car Model

1. Introduction

Optimizing an automobile's suspension system is essential for isolating passengers from road-induced vibrations and maximizing overall ride quality. Traditionally, engineers have relied on evolutionary optimization techniques, such as Genetic Algorithms (GAs), to determine the ideal suspension parameters like spring stiffness and damping coefficients. These algorithms systematically explore the design space to identify configurations that best minimize the vertical (heave) and pitching accelerations of the vehicle's chassis. [Xue et al. 2023; Mitra et al. 2016; Jabeen 2013]

Despite their robust optimization capabilities, evolutionary algorithms present significant computational hurdles. Accurately assessing vehicle dynamics typically requires running complex, simulations that account for various physical non-linearities. GAs evaluates thousands of potential design iterations before converging on an optimal solution, the overall process becomes exceedingly demanding in terms of both time and computational labour.

To circumvent these processing bottlenecks, combining surrogate modelling with NSGA-II offers a highly efficient alternative methodology. Rather than repeatedly executing full-scale simulations, a surrogate model acts as a lightweight, mathematical approximation of the system. By applying techniques like Gaussian Process regression to a small, initial dataset

derived from the expensive simulations, the surrogate can reliably predict the complex relationships between the suspension design variables and the resulting ride comfort. Consequently, this predictive approach enables engineers to achieve precise suspension tuning while drastically reducing the required computational load. [Jin 2011; Ribaud 2020]

While surrogate-assisted multi-objective optimization has been applied to suspension design, it is concentrated predominantly on quarter-car [Salem 2018; Nagarkar et al. 2019; Mudduluru 2021], which captures only vertical dynamics and cannot represent the coupling between front and rear axle motion. Half-car studies do account for pitch dynamics but have generally relied on direct genetic-algorithm search rather than surrogate-accelerated optimization and have pitch as a state variable within a combined comfort index rather than treating it as an independent, co-optimized objective [Mirzaei et al. 2007; Bhunia et al. 2011; Goga and Kľúčik 2012]. This study addresses that gap by coupling surrogate modelling with NSGA-II on a half-car model, formulating heave and pitch acceleration as two explicitly balanced objectives rather than optimizing heave in isolation.

2. Mathematical Model for Two-Wheeler Suspension

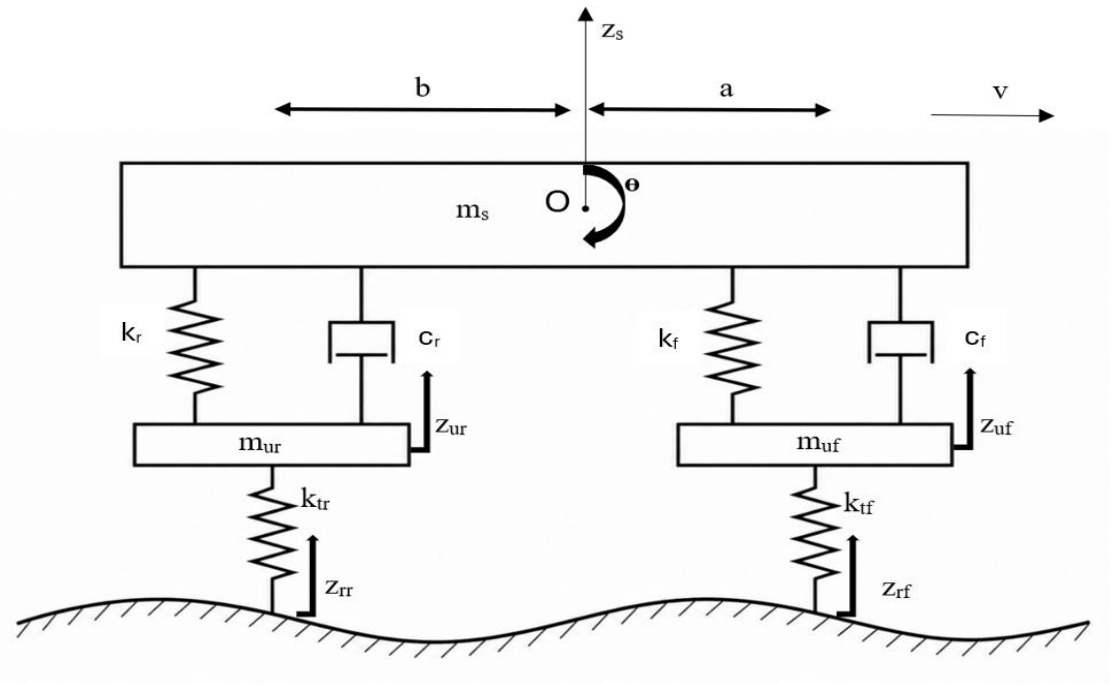

Figure 1: Half Car Model

Consider a two-wheeler modeled as a half car model. The half car is subjected to road excitations when the vehicle moves with velocity 'v'. The equations of motions of the vehicle body that dictates it dynamics are given by:

$$m_s\ddot{z_s} + k_f(z_s - a\theta - z_{uf}) + k_r(z + b\theta - z_{ur}) + c_f(\dot{z_s} - a\dot{\theta} - \dot{z_{uf}}) + c_r(\dot{z_s} + b\dot{\theta} - \dot{z_{ur}}) = 0 \quad (1)$$

$$I_y\ddot{\theta} + k_f a(z_s - a\theta - z_{uf}) + k_r b(z + b\theta - z_{ur}) - c_f a(\dot{z_s} - a\dot{\theta} - \dot{z_{uf}}) + c_r b(\dot{z_s} + b\dot{\theta} - \dot{z_{ur}}) = 0 \quad (2)$$

$$m_{uf}\ddot{z_{uf}} - k_f(z_s - a\theta - z_{uf}) + c_f(\dot{z_{uf}} + a\dot{\theta} - \dot{z_s}) - k_{tf}(z_{rf} - z_{uf}) = 0 \quad (3)$$

$$m_{ur}\ddot{z_{ur}} - k_r(z_s + b\theta - z_{ur}) - c_r(\dot{z_s} - b\dot{\theta} - \dot{z_{ur}}) - k_{tr}(z_{rr} - z_{ur}) = 0 \quad (4)$$

where m_s is the sprung mass, m_{uf} is the front unsprung mass, m_{ur} is the rear unsprung mass, and I_y is the pitching moment of inertia of sprung mass. The vertical displacements of the sprung mass, front unsprung mass, and rear unsprung mass are denoted by z_s, z_{uf} and z_{ur}, respectively. The angular displacement of the sprung mass about its center of gravity is represented by θ, while a and b denote the distances from the CG to the front and rear axles, respectively. The road excitation inputs acting on the front and rear wheels are represented by z_{rf} and z_{rr}, respectively.

The first and second-time derivatives of displacement denote velocity and acceleration. Accordingly, $\dot{z_s}$ and $\ddot{z_s}$ represent the velocity and acceleration of the sprung mass, $\dot{z_{uf}}$ represents the velocity of the front unsprung mass, and $\dot{z_{ur}}$ and $\ddot{z_{ur}}$ represent the velocity and acceleration of the rear unsprung mass, respectively. Similarly, $\dot{\theta}$ and $\ddot{\theta}$ denote the angular velocity and angular acceleration of the sprung mass about its center of gravity.

The front and rear suspension stiffnesses are denoted by k_f and k_r, respectively, while k_{tf} and k_{tr} represent the front and rear tyre stiffnesses. The damping coefficients of the front and rear suspensions are represented by c_f and c_r, respectively.

Rewriting the equation 1-4 in state space form:

$$X = [z_s, \theta, z_{uf}, z_{ur}] \quad (5)$$

$$M = \begin{bmatrix} m_s & 0 & 0 & 0 \\ 0 & I_y & 0 & 0 \\ 0 & 0 & zuf & 0 \\ 0 & 0 & 0 & zur \end{bmatrix} \quad (6)$$

$$K = \begin{bmatrix} k_f + k_r & -k_f a + k_r b & -k_f & -k_r \\ -k_f a + k_r b & k_f a^2 + k_r b^2 & k_f a & -k_r b \\ -k_f & k_f a & k_f + k_{tf} & 0 \\ -k_r & -k_r b & 0 & k_r + k_{tr} \end{bmatrix} \quad (7)$$

$$C = \begin{bmatrix} c_f + c_r & -c_f a + c_r b & -c_f & -c_r \\ -c_f a + c_r b & c_f a^2 + c_r b^2 & c_f a & -c_r b \\ -c_f & c_f a & c_f & 0 \\ -c_r & -c_r b & 0 & c_r \end{bmatrix} \quad (8)$$

$$K_t = \begin{bmatrix} 0 & 0 \\ 0 & 0 \\ k_{tf} & 0 \\ 0 & k_{tr} \end{bmatrix} \quad (9)$$

$$U = \begin{bmatrix} z_{rf} \\ z_{rr} \end{bmatrix} \tag{10}$$

$$M\ddot{X} + C\dot{X} + KX = K_t U \tag{11}$$

$$x = \begin{bmatrix} X \\ \dot{X} \end{bmatrix} \tag{12}$$

$$\dot{x} = \begin{bmatrix} \dot{X} \\ \ddot{X} \end{bmatrix} \tag{13}$$

$$\dot{x} = \begin{bmatrix} 0 & I \\ -M^{-1}K & -M^{-1}C \end{bmatrix} \begin{bmatrix} X \\ \dot{X} \end{bmatrix} + \begin{bmatrix} 0 \\ M^{-1}K_t \end{bmatrix} U \quad \text{where } I = \begin{bmatrix} 1 & 0 & 0 & 0 \\ 0 & 1 & 0 & 0 \\ 0 & 0 & 1 & 0 \\ 0 & 0 & 0 & 1 \end{bmatrix} \tag{14}$$

Vehicle Parameters	Values [Units]
m_s	275 kg
m_{uf}	12 kg
m_{ur}	17 kg
I_y	87.56 kg.m^2
a	0.918 m
b	0.472 m
k_{tf}	100000 N/m
k_{tr}	100000 N/m
v	10 m/s

Table 1: Vehicle Parameters

3. Road Profile Generation

To accurately simulate real-world driving conditions, the road surface excitation is modeled as a Gaussian random process in accordance with the ISO-8608 standard [ISO:8608 2016]. The road profile is defined in the spatial frequency domain using a Power Spectral Density (PSD) function. For an average road categorized as Class-C, the spatial PSD is mathematically expressed as:

$$G_d(n) = G_d(n_0)\left(\frac{n}{n_0}\right)^{-w} \tag{15}$$

where n represents the spatial frequency (cycles/m), $n_0 = 0.1$ cycles/m is the reference spatial frequency, $G_d(n_0) = 256 \times 10^{-6}\, m^3$ denotes the reference degree of roughness specific to a Class-C profile, and $w = 2$ is the standard waviness exponent.

The numerical integration of the 4-DOF equivalent model requires continuous time-domain inputs, the spatial PSD must be transformed into a dynamic time history. This is achieved utilizing the superposition of harmonics method as detailed in [ISO:8608 2016]. The continuous spatial frequency spectrum is discretized into a finite number of frequency bands,

and the road elevation is constructed by summing a series of sinusoidal waves, each assigned a uniformly distributed random phase angle. The vehicle's constant longitudinal velocity serves as the critical parameter for the mathematical mapping of the spatial frequencies (n) into temporal frequencies. Furthermore, to accurately capture the specific pitch and bounce dynamics of the two-wheeler, the time-domain road disturbance applied to the rear tire is modeled using an explicit time delay relative to the front tire, derived directly from the vehicle's wheelbase and forward velocity.

$$\Delta n = \frac{n_{max} - n_{min}}{N} \tag{16}$$

$$n_i = n_{min} + \left(i - \frac{1}{2}\right)\Delta n \quad \text{i=1,2,3…. N} \tag{17}$$

$$A_i = \sqrt{2\ G(n_i)\Delta n} \tag{18}$$

$$z_{rf}(t) = \sum_{i=1}^{N} \sqrt{2\ G(n_i)\Delta n}\ \cos(2\pi n_i v t\ + \varphi_i) \tag{19}$$

$$z_{rr}(t) = \sum_{i=1}^{N} \sqrt{2\ G(n_i)\Delta n}\ \cos(2\pi n_i v (t - \Delta t)\ + \varphi_i) \tag{20}$$

$$\Delta t = \frac{a+b}{v} \tag{21}$$

4. Surrogate Modeling Methodology

4.1 Design of Experiments and Data Generation

To construct a robust and accurate surrogate model, the multi-dimensional design space must be systematically sampled. Latin Hypercube Sampling (LHS) was employed to generate an initial matrix of suspension parameter combinations, specifically bounding the front and rear spring stiffness (k_f, k_r) and damping coefficients (c_f, c_r)[Hiranga and Shiiba 2004; Chen et al.2015]. Highest allowable sag and preloads were used to calculate the upper and lower bounds of suspension parameters. The limits were relaxed to eliminate all chances of overstraining of design space. LHS was selected because it guarantees a stratified, and near uniform space filling distribution across all parameter bounds, preventing data clustering and ensuring the surrogate captures the global non-linear behavior of the system. [Simpson et al. 2001]

For each parameter combination generated by the LHS, the 4-DOF half-car mathematical model was numerically integrated in MATLAB. Each simulation was run for a duration of 300 seconds, utilizing the transformed time-domain ISO-8608 Class-C Road excitation. From each 300-second dynamic evaluation, four critical performance metrics were extracted to serve as the training targets for the surrogate:

1. RMS Heave Acceleration: To quantify vertical ride comfort.
2. RMS Pitch Acceleration: To quantify rotational ride comfort.
3. Maximum Rider Sag: To evaluate baseline vehicle stance constraints.
4. Maximum Dynamic Suspension Displacement: To ensure the suspension operates within its physical travel limits.

Parameters	Lower Bound	Upper Bound
Front Suspension Stiffness	4000 [N/m]	30,000 [N/m]
Front Suspension Damping	100 [Ns/m]	2000 [Ns/m]
Rear Suspension Stiffness	10000 (N/m)	65000 [N/m]
Rear Suspension Damping	200 (Ns/m)	4100 [Ns/m]

Table 2: Bounds of NSGA-II Algorithm

4.2 Surrogate Construction

To bypass the computational bottleneck of the continuous 300-second numerical integrations, the data generated by the LHS and MATLAB solver was used to train Gaussian Process Regression (GPR) model, commonly referred to as Kriging.

The surrogate was constructed utilizing an Automatic Relevance Determination (ARD) squared exponential kernel function. The ARD kernel is highly advantageous for complex vehicle dynamics because it assigns distinct length scales to each individual input dimension [Rasmussen and Williams 2006]. This allows the model to determine and scale the relative influence of front versus rear stiffness and damping on the resulting vehicle accelerations and displacements, yielding a highly tuned predictive surface.

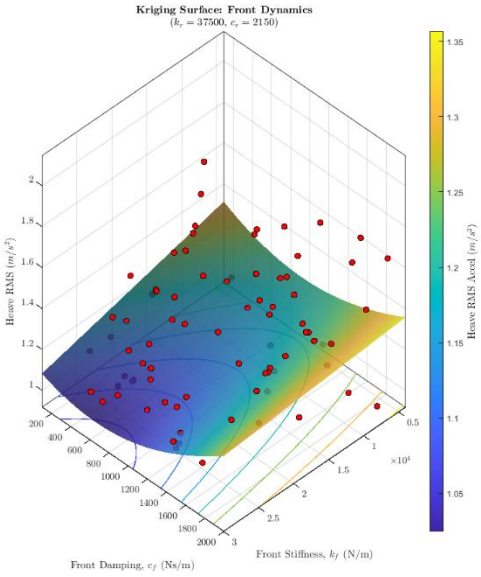

Figure 2: Kriging Surface for heave acceleration with respect to front stiffness and damping

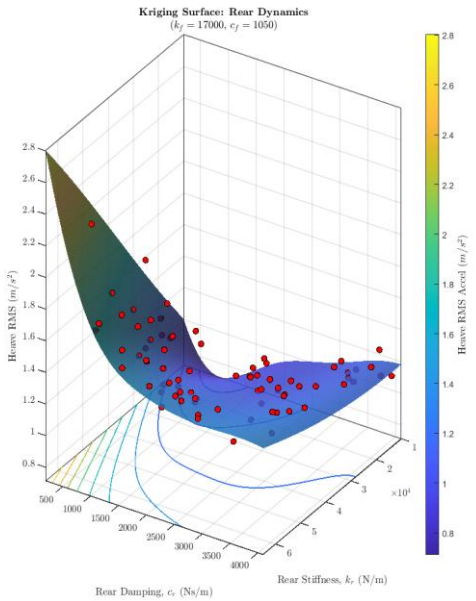

Figure 3: Kriging Surface for heave acceleration with respect to rear stiffness and damping

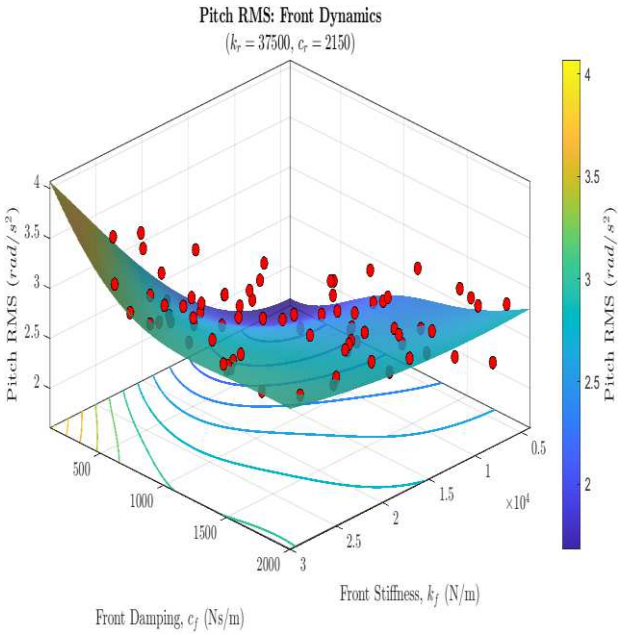

Figure 4: Kriging Surface for Pitching Acceleration with respect to front suspension stiffness and damping

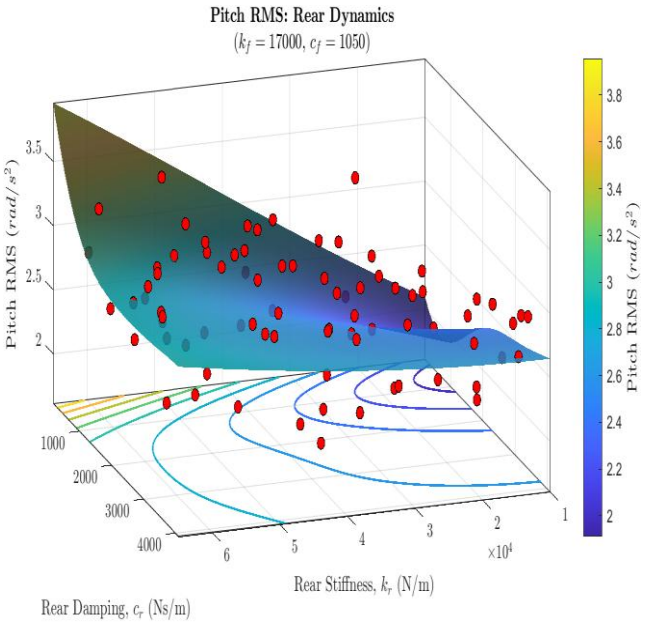

Figure 5: Kriging Surface for Pitching Acceleration with respect to rear suspension stiffness and damping

The complete Kriging response surface exists in a 5-dimensional space, direct visualization is impossible. To visually assess the gradient topography and non-linearities captured by the surrogate model, 3D cross-sectional slices were generated (Figure 2-Figure5). For the front suspension topography, the rear stiffness and damping variables were held constant within their respective Latin Hypercube design bounds ($k_r = 37500$N/m, $c_r = 2150$ Ns/m), and vice versa for the rear topography.

4.3 Surrogate Validation

The out-of-sample validation results demonstrated strong predictability across both the primary optimization objectives and physical constraints. As illustrated in Figure 6, the R^2 score for the surrogate model of Heave was 0.9804, while the R^2 score of Pitch is 0.9149. Similarly, the R^2 score of Front and Rear Travel is 0.9982 and 0.9454 respectively.

This predictiveness is shown by the scatter plots in Figure 6 to Figure-9, where the tight alignment of the validation data along the ideal $y = x$ reference line demonstrates the strict bounds of the prediction error across all four metrics. Therefore, the surrogate framework can be deemed validated for the multi-objective optimization phase.

Overall, the Kriging algorithm successfully captured 91% of the variance across the objective space, ensuring the NSGA-II algorithm navigates a mathematically sound fitness topology. Furthermore, evaluating the absolute physical error reveals the true robustness of the constraint models: the RMSE values for Maximum Front and Rear Travel are exceptionally low at 0.375 mm and 1.8 mm. From a vehicle dynamics perspective, a predictive margin of error of less than 2 mm is acceptable for enforcing boundary constraints against the 100 mm front and 50 mm rear stroke limits.

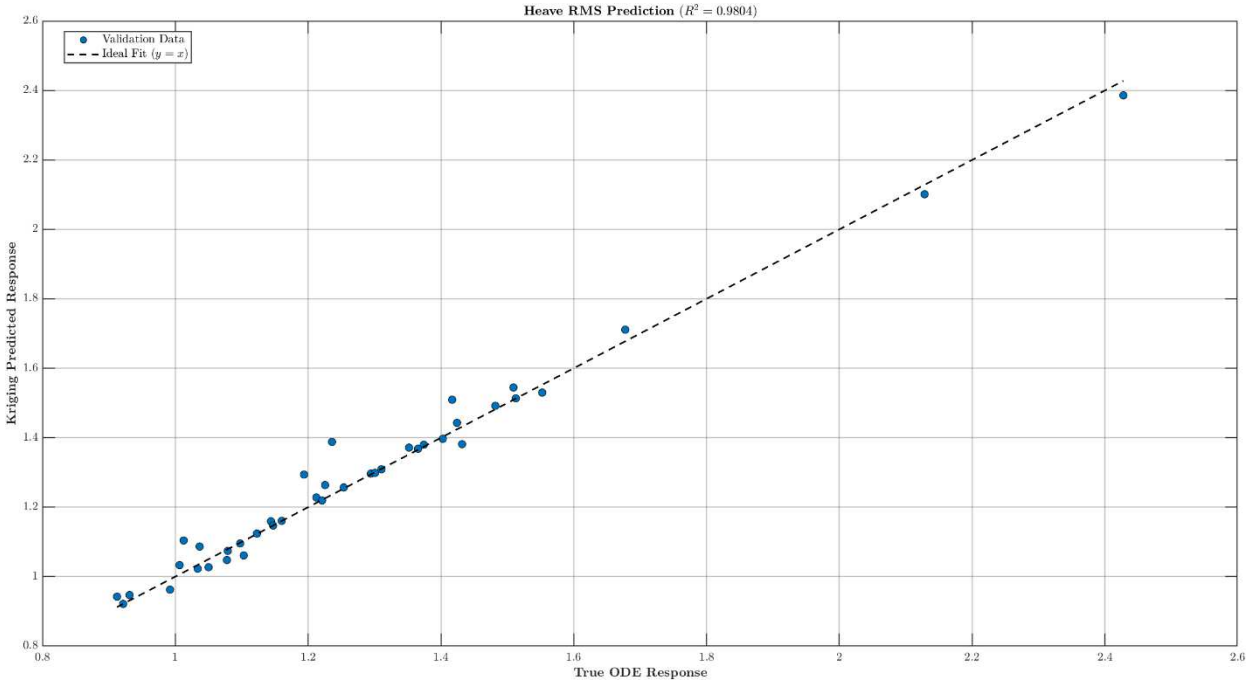

Figure 6: Correlation of Kriging and ODE solver for vertical acceleration.

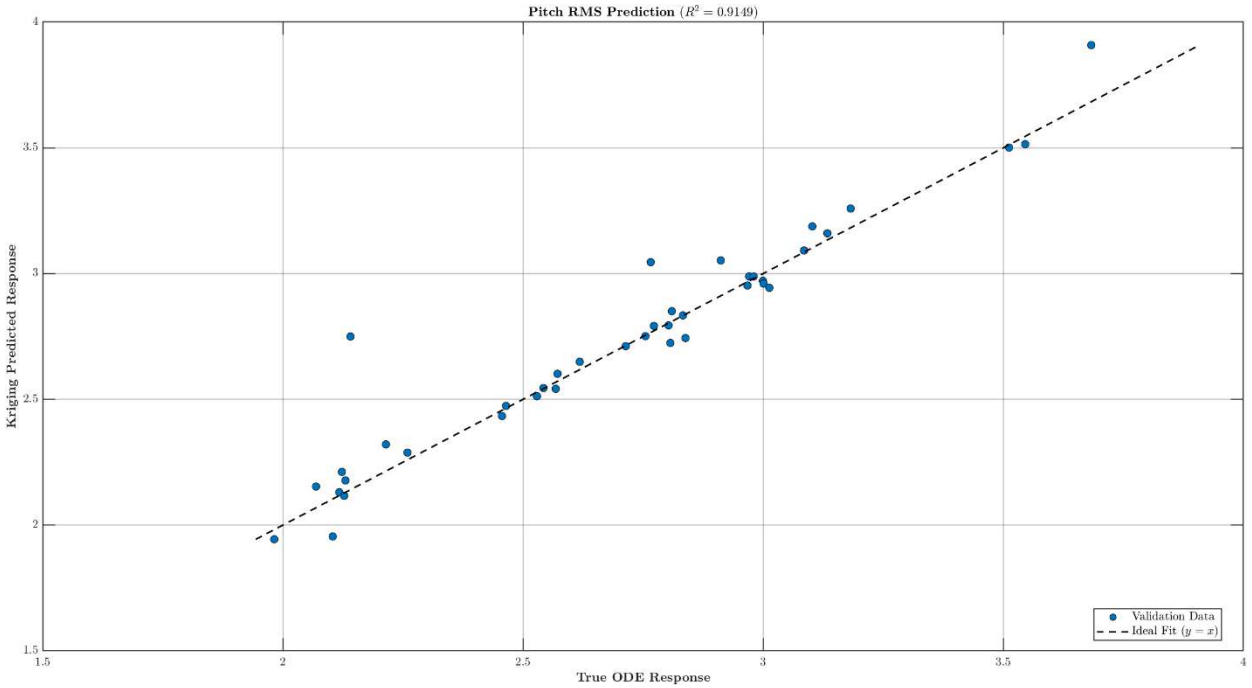

Figure 7: Correlation of Kriging and ODE solver for pitching acceleration.

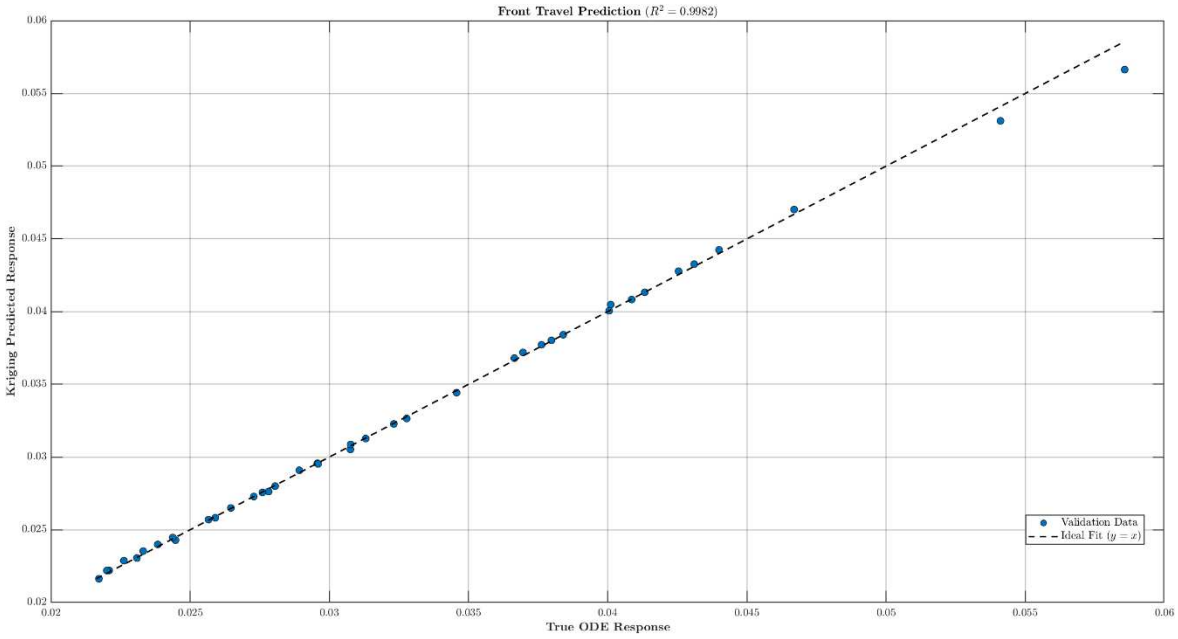

Figure 8: Correlation of Kriging and ODE solver for front suspension travel

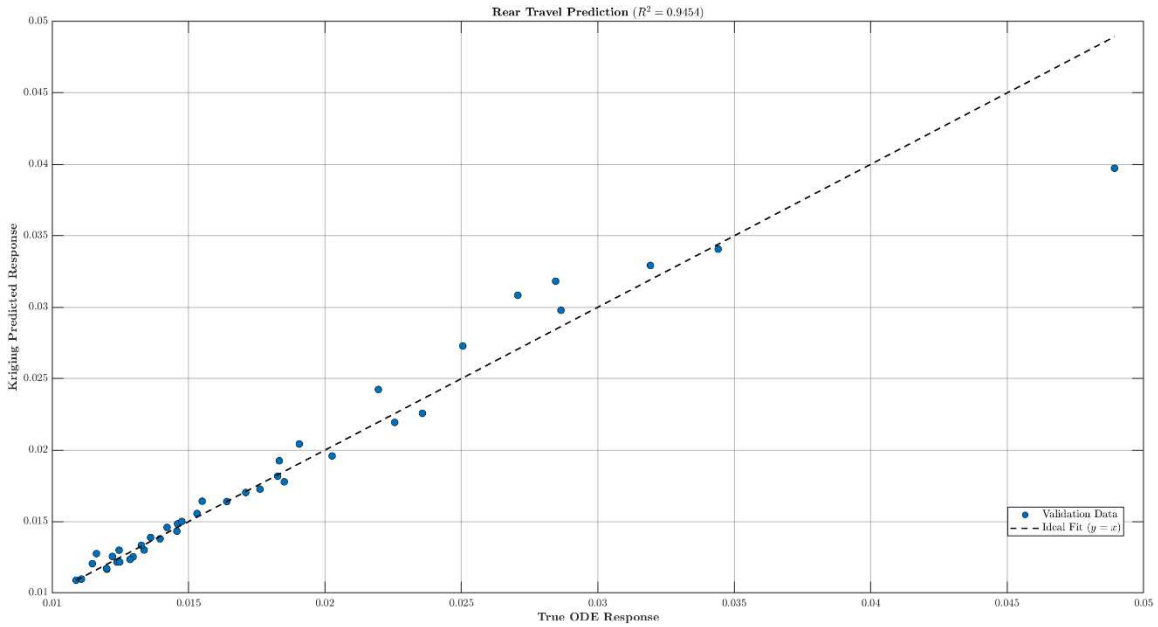

Figure 9: Correlation of Kriging and ODE solver for rear suspension travel

5. Multi-Objective Optimization

5.1 Problem Formulation

The optimization of the two-wheeler suspension system is formulated as a constrained multi-objective problem. The goal is to maximize rider comfort by minimizing both the vertical (heave) and rotational (pitch) accelerations of the sprung mass, while strictly adhering to physical vehicle constraints.

Let the design vector be defined as the front and rear suspension parameters:

$$\mathbf{x} = \left[k_f, k_r, c_f, c_r\right]^T \quad (22)$$

The multi-objective optimization problem is mathematically expressed as:

$$\textbf{Minimize } F(\mathrm{x}) = [f_1(\mathrm{x}), f_2(\mathrm{x})]^T \quad (23)$$

Here, $f_1(x)$ is RMS of heave acceleration and $f_2(x)$ is the RMS of pitching acceleration.

The optimization is subjected to the following physical and dynamic constraints to ensure safe vehicle stance and adequate road-holding capability:

$$g_1(\mathbf{x}) = \mathrm{Sag}_{rider}(\mathbf{x}) - \mathrm{Sag}_{allowable} \leq 0 \quad (24)$$

$$g_2(\mathbf{x}) = Z_{sus,max}(\mathbf{x}) - Z_{travel,limit} \leq 0 \quad (25)$$

$\mathbf{x}^{(L)} \leq \mathbf{x} \leq \mathbf{x}^{(U)}$ (where, L and U denote the lower and upper bounds of the parameters). (26)

Under the maximum load condition (vehicle sprung mass, a 75 kg rider, and a 75 kg pillion), the allowable rider sag is limited to 60% of the 100 mm front suspension stroke and 65% of the 50 mm rear suspension stroke. The suspension preload is fixed at 25 mm for the front and 18 mm for the rear.

5.2 Integration of NSGA-II Algorithm with Surrogate Surface.

To resolve the inherently conflicting nature of the objective functions, where minimizing vertical acceleration requires a softer suspension that consequently degrades pitch stability and consumes dynamic travel, the NSGA-II is implemented [Jones et al. 1998; Konak et al. 2006]. NSGA-II is highly effective for balancing conflicting engineering design objectives, as it utilizes a fast non-dominated sorting approach and maintains population diversity through crowding distance calculations, ultimately yielding a well-distributed Pareto optimal front. For this study, the algorithm was configured with a population size of 200 and evolved over 200 generations. Furthermore, to facilitate a robust exploration of the global design space, the crossover fraction was set to 0.8.

Within the genetic algorithm, each candidate solution represents a unique suspension parameter configuration whose corresponding heave and pitch responses must be evaluated. The critical advantage of this framework lies in the fitness evaluation phase, where the RMS heave and RMS pitch metrics are evaluated by directly querying the validated surrogate surface rather than utilizing the full differential equation solver [Yagoubi and Bederina 2023]. This entirely bypasses bottleneck of transient time-domain calculations, allowing NSGA-II to evaluate tens of thousands of candidate configurations in a fraction of the time, thereby mapping the Pareto optimal solutions with extreme computational efficiency.

6. Results and Discussion

6.1 Pareto Front Analysis and Physical Trade-offs

The deployment of the NSGA-II algorithm across the Kriging surrogate model successfully yielded a well-defined Pareto optimal front. The nature of these non-dominated set of solutions

illustrates the inherent physical conflict in two-wheeler suspension tuning: the direct trade-off between minimizing vertical heave acceleration (Objective 1) and minimizing rotational pitch acceleration (Objective 2).

The physical meaning of this curve is rooted in the vehicle's coupled dynamics. Solutions located at the extreme end favoring minimal heave acceleration (achieving a minimum ($f_1 \approx 1.03\ m/s^2$) typically drive the front stiffness and damping (k_f, c_f) parameters and toward their highest allowable bounds, and rear stiffness and damping parameters (k_r, c_r) to their lowest allowable settings. While this effectively isolates the sprung mass from vertical road inputs, this configuration severely under-damps the rotational modes, leading to a high maximum pitch response ($f_2 \approx 2.76\ rad/s^2$) when the front and rear tires encounter the same road disturbance with a time delay.

Conversely, selecting a solution at the opposite extreme that strictly minimizes pitch (achieving a minimum $f_2 \approx 1.97$) requires stiffer parameter configurations on the rear suspension. This inherently transmits more high-frequency vertical vibration directly to the rider, maximizing the heave acceleration ($f_1 \approx 1.09$).

This generated Pareto front allows for the precise selection of a balanced configuration like that of near $f_1 \approx 1.05$ and $f_2 \approx 2.27$, that balances these modes without violating the maximum sag and suspension travel constraints.

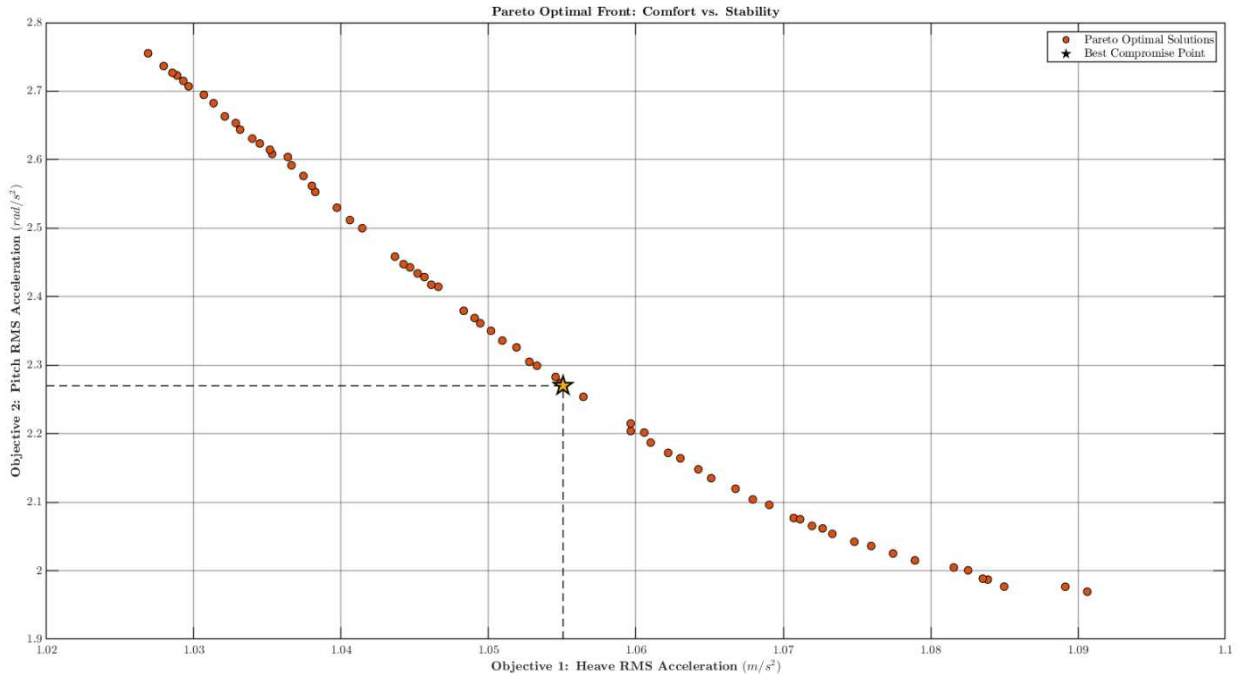

Figure 10: Pareto Front

6.2 Computational Efficiency

The primary objective of this study was to bypass the computational bottleneck associated with multi-body numerical integrations during the optimization phase. To quantify this improvement, the computational expense of the surrogate-assisted framework was directly compared to a theoretical traditional approach.

In a standard optimization loop, evaluating a population 200 over 200 generations equates to 40,000 independent fitness evaluations. Using the 4-DOF MATLAB model, a single 300-second dynamic simulation requires approximately 0.4802 seconds to solve. Therefore, the traditional method would necessitate an estimated 5.3 hours of continuous computing time.

In contrast, evaluating those same 40,000 design iterations using the trained Kriging model required only 45.84 seconds. The proposed methodology achieved a total computational time reduction of over 419% conclusively validating the efficiency of the surrogate framework.

6.3 Time-Domain Verification

To ensure that the mathematical optimum identified by the surrogate model translates to actual physical performance, a balanced solution from the center of the Pareto front (designated as the "Best Compromise Point") was subjected to time-domain verification.

The parameter values of this optimum (k_f =14934 N/m, c_f = 571 Ns/m, k_r=35329 Ns/m, c_r = 1999 Ns/m) were fed back into the original, continuous 4-DOF MATLAB dynamic simulation and evaluated over the ISO-8608 Class-C Road profile. The resulting time-history responses of the sprung mass were plotted alongside a baseline, unoptimized suspension configuration (k_{fd} =12628 N/m, c_{fd} = 424 Ns/m, k_{rd}=44000Ns/m, c_{rd} = 1200 Ns/m).

The comparative time-domain analysis physically verified the surrogate's predictions. The optimal configuration demonstrated significant attenuation in peak transient accelerations and a faster settling time following large road disturbances. The optimal configuration reduced RMS heave acceleration by 16% (1.32 → 1.10 m/s²) and RMS pitch acceleration by 0.6% (2.27 → 2.25 m/s²) relative to baseline. Furthermore, maximum dynamic displacement data confirmed that the optimized setup safely utilized the available working space without bottoming out, proving that the algorithm successfully enhanced rider comfort while strictly adhering to kinematic safety boundaries.

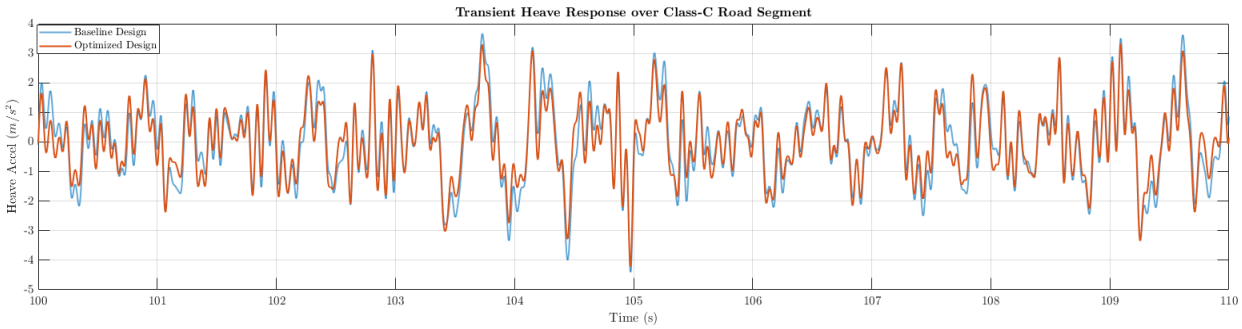

Figure 11: Transient heave response of the sprung mass: a 10-second comparison of the baseline versus the optimized suspension design.

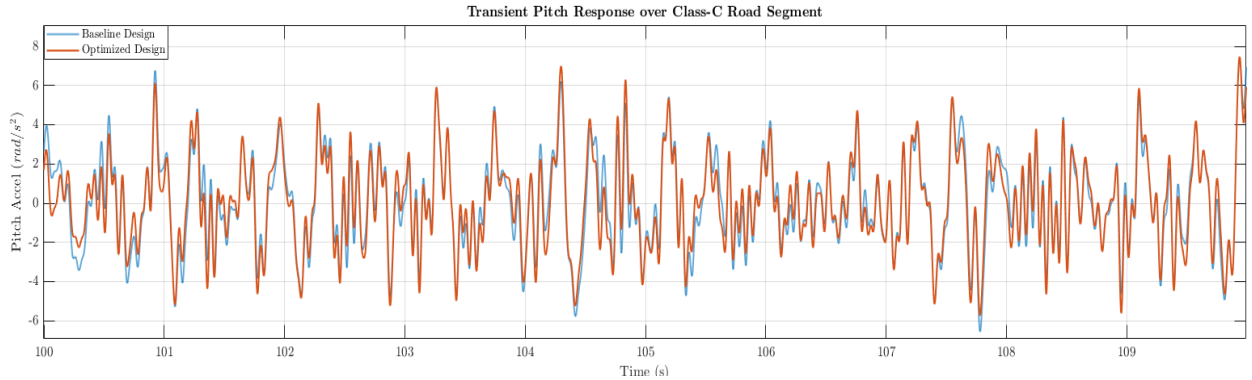

Figure 12: Transient pitch response of the sprung mass: A 10-second comparison of the baseline versus the optimized suspension design.

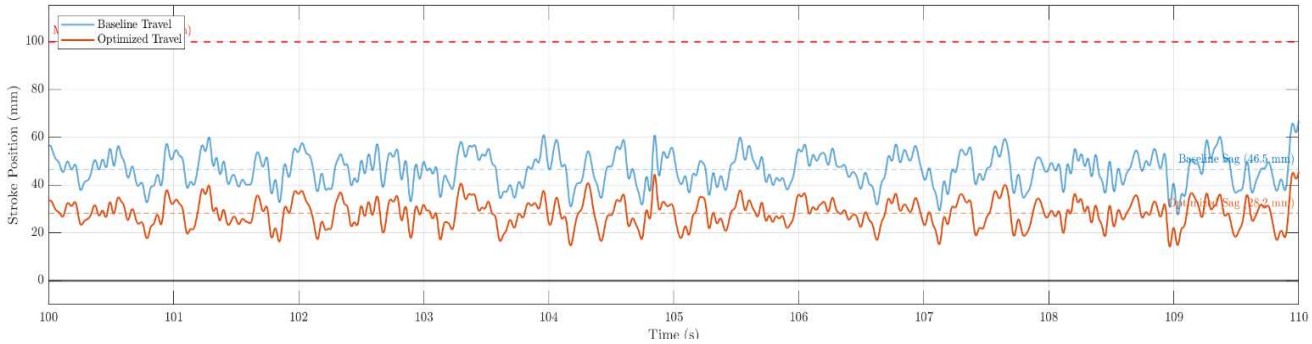

Figure 13: Time-domain comparison of the front suspension absolute travel (dynamic deflection plus static sag) for the baseline and optimized configurations over a 10-second transient window.

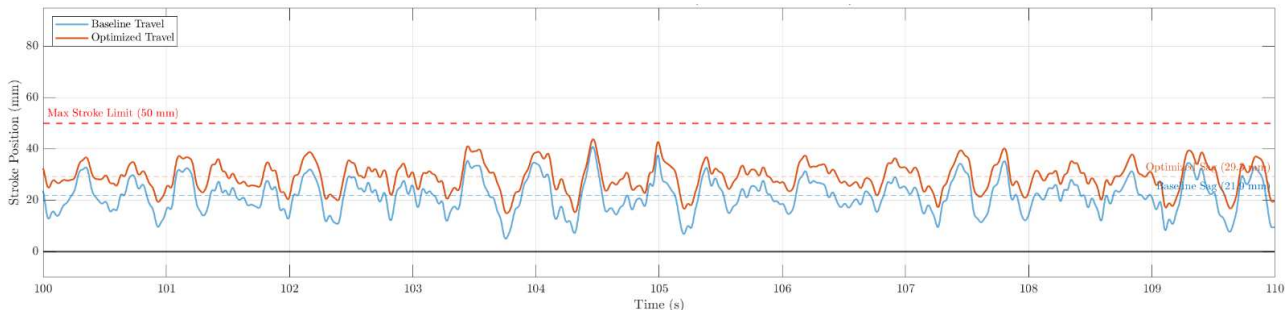

Figure 14: Time-domain comparison of the front suspension absolute travel (dynamic deflection plus static sag) for the baseline and optimized configurations over a 10-second transient window.

7. Conclusion:

This study successfully developed and validated a computationally efficient framework for the multi-objective optimization of a two-wheeler suspension system. By replacing the time-intensive numerical integration of a 4-DOF half-car dynamic model with a high-fidelity surrogate model, the inherent computational bottlenecks of traditional vehicle dynamics optimization were effectively bypassed. Utilizing Latin Hypercube Sampling (LHS) and Gaussian Process Regression (Kriging) equipped with an ARD squared exponential kernel, a robust predictive surface was generated to map the non-linear relationship between suspension parameters and vehicle dynamic responses over an ISO-8608 Class-C Road profile.

The integration of this Kriging surrogate with the NSGA-II algorithm yielded a well-defined negative gradient Pareto optimal front proving a conflictive relationship between pitch (rotational stability) and heave acceleration (riding comfort). The proposed framework allowed

for selection of a balanced, optimal suspension configuration that balances these vertical and rotational modes without violating essential constraints regarding sag and maximum dynamic suspension travel.

Most notably, the surrogate-assisted methodology achieved a computational time reduction of over 419% compared to traditional continuous MATLAB evaluations, processing thousands of design iterations in a fraction of the time. Time-domain verification further confirmed that the mathematically optimal configuration translates to a tangible physical improvement, demonstrating a significant reduction in peak transient accelerations compared to the baseline setup.

Future work will focus on extending this surrogate-assisted framework to a high-fidelity dynamic model, incorporating severe non-linearities such as progressive spring rates and dual-stage damping, and validating the computational findings against physical empirical data utilizing a hydraulic test rig. Human sensitivity to vibration frequency as defined in ISO-2631 will be included to better tuning of suspension.

8. Data Availability Statement

The MATLAB scripts used for the 4-DOF half car model, Latin Hypercube Sampling training datasets, and the validated Kriging surrogate models generated during this study are available from the corresponding author upon reasonable request.

9. Generative AI Declaration

Generative AI was used strictly for grammatical refinement during the drafting of this manuscript.

10. Conflict of Interest

There is no conflict of interest with any parties related to this research article.

11. Funding Declaration

No external funding has been received for this study.

Reference:

1. Xue, H.; Gobbi, M.; Matta, A. Multi-fidelity surrogate-based optimal design of road vehicle suspension systems. Optimization and Engineering, 24, 2773–2794 (2023). https://doi.org/10.1007/s11081-023-09793-0
2. Mitra, A.C.; Desai, G.J.; Patwardhan, S.R.; Shirke, P.H.; Kurne, W.M.H.; Banerjee, N. Optimization of passive vehicle suspension system by genetic algorithm. Procedia Engineering. 144. 1158-1166. doi:10.1016/jroeng.2016.05.087
3. Jabeen, S.D. Vibration optimization of a passive suspension system via genetic algorithm. International Journal of Modelling, Simulation and Scientific Computing, 4(1) (2013). https://doi.org/10.1142/S1793962312500225
4. Jin, Y. Surrogate-assisted evolutionary computation: Recent advances and future challenges. Swarm and Evolutionary Computation, 1(2), 61–70 (2011). https://doi.org/10.1016/j.swevo.2011.05.001

5. Ribaud, M.; Blanchet-Scalliet, C.; Helbert, C.; Gillot, F. Robust optimization: A kriging-based multi-objective optimization approach. Reliability Engineering & System Safety, 200, 106913 (2020). https://doi.org/10.1016/j.ress.2020.106913
6. Salem, M.H. Investigation of a non-linear suspension in a quarter car model. [Doctoral Dissertation] (2018).
7. Nagarkar, M.P.; El-Gohary, M.A.; Bhalerao, Y.J.; et al. Artificial neural network prediction and validation of optimum suspension parameters of a passive suspension system. SN Applied Sciences, 1, 569 (2019). https://doi.org/10.1007/s42452-019-0550-0
8. Mudduluru, S.R.; Chizari, M. Quarter and full car models optimization of passive and active suspension system using genetic algorithm. arXiv:2101.12629 (2021).
9. Mirzaei, M.; Hassannejad, R. Application of genetic algorithms to optimum design of elasto-damping elements of a half-car model under random road excitations. Proceedings of the Institution of Mechanical Engineers, Part K: Journal of Multi-body Dynamics, 221(4), 515–526 (2007). https://doi.org/10.1243/14644193JMBD101
10. Bhunia, A.; Jabeen, S.; Mukherjee, R.N. Vibration control of a vehicle using region reduction division criteria. International Journal of Materials and Structural Integrity, 5, 311–332 (2011). https://doi.org/10.1504/IJMSI.2011.044419
11. Goga, V.; Kľúčik, M. Optimization of vehicle suspension parameters with use of evolutionary computation. Procedia Engineering, 48, 174–179 (2012). https://doi.org/10.1016/j.proeng.2012.09.502
12. ISO 8608:2016. Mechanical Vibration — Road Surface Profiles — Reporting of Measured Data. International Organization for Standardization (2016).
13. Hiraga, T.; Shiiba, T. Surrogate modelling of suspension with high stiffness element for real-time analysis using machine learning. 16th International Symposium on Advanced Vehicle Control, 399-405. (2004)
14. Chen, S.; Shi, T.; Wang, D.; Chen, J. Multi-objective optimization of vehicle ride comfort based on Kriging approximate model and NSGA-II. Journal of Mechanical Science and Technology. https://doi.org/10.1007/s12206-015-0215-x
15. Simpson, T.W.; Peplinski, J.; Koch, P.N.; Allen, J.K. Meta-models for computer-based engineering design: Survey and recommendations. Engineering with Computers, 17(2), 129–150 (2001).
16. Rasmussen, C.E.; Williams, C.K.I. Gaussian Processes for Machine Learning. MIT Press, pp. 106–108 (2006).
17. Jones, D.R.; Schonlau, M.; Welch, W.J. Efficient global optimization of expensive black-box functions. Journal of Global Optimization, 13, 455–492 (1998). https://doi.org/10.1023/A:1008306431147
18. Konak, A.; Coit, D.W.; Smith, A.E. Multi-objective optimization using genetic algorithms: A tutorial. Reliability Engineering and System Safety, 91(9), 992–1007 (2006).
19. Yagoubi, M.; Bederina, H. Surrogate-assisted NSGA-II algorithm for expensive multi-objective optimization. Proceedings of the Genetic and Evolutionary Computation Conference (GECCO 2023) (2023). https://doi.org/10.1145/3583133.3590746